

The use of thermodynamic excess functions in the Nernst distribution law

NORMAN B. HOLST, JR.

Department of Geological Sciences, University of Illinois
Chicago, Illinois 60680

Abstract

The Nernst distribution law, which is used by many authors in geology as the theoretical basis of geothermometry and trace-component distribution, is derived using excess functions. It is demonstrated that the free-energy term in the Nernst equation, as it is applied in many of these cases, is an excess function and describes the non-ideal behavior of the phases involved. It is then not necessary to introduce any assumptions concerning activities or activity coefficients, and one may use simple mole fractions instead. Analysis of system data in light of this allows one to make useful predictions concerning the accuracy of the data and the behavior of the system at elevated temperatures. Analysis is made of various data on the diopside-enstatite solvus as an example.

The Nernst distribution equation is a very useful theoretical basis for approaching geothermometry and trace-component distribution. The derivation of the Nernst equation is dependent on the convention one uses for dealing with non-ideality in solutions. There are two common conventions: activities, and thermodynamic excess functions.

There are two systems of activities (Castellan, 1971): the rational system using Raoult's law as the limiting case (activity coefficient approaches 1 as mole fraction approaches 1); and the practical system using Henry's law as the limiting case (activity coefficient approaches 1 as mole fraction approaches 0). Activities are more commonly used in geological literature, but excess functions would be more effective and eliminate confusion in some instances. A more complete discussion of thermodynamic excess functions can be found in Thompson (1967) or Swalin (1972). This paper will deal only with their application to the Nernst distribution equation.

Thermodynamic excess functions can be defined as the thermodynamic functions of real solutions minus the respective functions of ideal solutions. Thus the excess chemical potential of component 1 in phase A is the actual chemical potential of component 1 minus the chemical potential one would calculate if A were a perfect solution.

$$\mu_1^{Axs} = \mu_1^A - \mu_1^A(\text{ideal}) \quad (1)$$

Since there are two systems of activities, there are two relations between activity and excess chemical potential. In the rational system:

$$\mu_1^A = \mu_1^p + RT \ln X_1^A + RT \ln \gamma_1^A \quad (2)$$

$$\mu_1^A(\text{ideal}) = \mu_1^p + RT \ln X_1^A \quad (3)$$

$$\mu_1^{Axs} = RT \ln \gamma_1^A \quad (4)$$

where γ is the activity coefficient, X is the mole fraction and μ_1^p is the chemical potential of pure 1. In the practical system:

$$\mu_1^A = \mu_1^p + RT \ln X_1^A + RT \ln K_1^A + RT \ln \gamma_1^A \quad (5)$$

$$\mu_1^{Axs} = RT \ln K_1^A + RT \ln \gamma_1^A \quad (6)$$

where K is the Henry's law constant and γ is again an activity coefficient.

The practical system of activities is usually used in working with dilute solutions and the rational system when working with more concentrated solutions. However, by deriving the Nernst distribution equation with excess functions one may work with either dilute or concentrated solutions without activities. If two phases (A and B) are in equilibrium, the chemical potential of any component (1) must be the same in each phase.

$$\mu_1^A = \mu_1^B \quad (7)$$

Combining either equations 2 and 4 in the rational

system or 5 and 6 in the practical system and substituting into equation 7 yields identical results:

$$\mu_1^A + RT \ln X_1^A + \mu_1^{Axs} = \mu_1^B + RT \ln X_1^B + \mu_1^{Bxs} \quad (8)$$

$$RT \ln (X_1^A/X_1^B) = -(\mu_1^{Axs} - \mu_1^{Bxs}) = -\Delta G^{xs}. \quad (9)$$

From this it is apparent that ΔG^{xs} is the change in excess free energy associated with the transfer of one mole of component 1 from phase B to A. Since ΔG^{xs} is an excess function, it describes the non-ideal behavior of the two solutions and it is not necessary to deal with activities in this form of the Nernst distribution law.

Pursuing this further let $K_p = (X_1^A/X_1^B)$; then

$$\ln K_p = -\frac{1}{R} \frac{\Delta G^{xs}}{T} \quad (10)$$

$$\frac{\partial \ln K_p}{\partial T} = -\frac{1}{R} \left[\frac{\partial(\Delta G^{xs}/T)}{\partial T} \right] \quad (11)$$

$$\frac{\partial \ln K_p}{\partial T} = -\frac{1}{R} \left[\frac{-\Delta H^{xs}}{T^2} \right] \quad (12)$$

$$\ln K_p = -\frac{1}{R} \int \frac{-\Delta H^{xs}}{T^2} \partial T \quad (13)$$

$$\ln K_p = -\frac{1}{R} \frac{\Delta H^{xs}}{T} + C. \quad (14)$$

For solid-state reactions ΔH and ΔS are almost constant over fairly broad temperature ranges (Swalin, 1972). If they do not vary greatly with the mole fraction of component 1 in each phase or if the degree of solution in each phase is small, then ΔH^{xs} and ΔS^{xs} can be considered constant. It can then be shown by statistical arguments (Swalin, 1972, p. 171) that $C = \Delta S^{xs}/R$; so that:

$$-RT \ln X_1^A/X_1^B = \Delta H^{xs} - T\Delta S^{xs}. \quad (15)$$

Therefore a plot of $\ln (X_1^A/X_1^B)$ versus $1/T$ should yield a straight line with a slope equal to $-\Delta H^{xs}/R$ and an intercept, at $1/T = 0$, equal to ΔS^{xs} . Approaches similar to this are often used as the theoretical basis for geothermometry (e.g. Carmichael *et al.*, 1974; Kern and Weisbrod, 1967; Wood and Banno, 1973) and trace component distribution (e.g. Broecker and Oversby, 1971). The approximation is usually made that activity equals mole fraction. On initial consideration this may seem to be a poor approximation, due to the very non-ideal behavior of these systems. In fact some authors are apologetic about using it (Wood and Banno, 1973). The above derivation of the Nernst equation demonstrates,

however, that the thermodynamic functions obtained by their plots or regressions are in fact excess functions and the non-ideal behavior is accounted for. Corrections for contaminants in the system may be made by empirically correcting ΔG^{xs} for its variation with phase composition.

Another useful plot is to calculate ΔG^{xs} as $-RT \ln (X_1^A/X_1^B)$ and plot this versus temperature. A linear regression run on the points should produce a straight line with a slope approximating $-\Delta S^{xs}$ and an intercept approximating ΔH^{xs} at $T = 0$. Actually the data points in this plot as well as the plot discussed in the previous paragraph will not fall on a straight line. This is because ΔH^{xs} and ΔS^{xs} do vary with temperature and phase composition. However, they should follow a smooth curve with no inflections or singular points. Inflections or singular points in ΔG curves and the corresponding discontinuities in the first-order derivatives (ΔH and ΔS) indicate a first-order transformation or reaction. Inflections or singular points in such plots are then good cause to suspect the accuracy of the data.

A good example is the geothermometer constructed by Wood and Banno (1973) from the diopside-enstatite phase diagram determined by Davis and Boyd (1966) at 30 kbar. There is a decided inflection in the diopside-rich limb of the Davis and Boyd solvus at about 1475°C and a corresponding inflection in the plot of $\ln(X_{Mg_2Si_2O_6}^{cpX}/X_{Mg_2Si_2O_6}^{opX})$ versus $1/T$. The Wood and Banno equation for the solvus was obtained by linear regression on the solvus data:

$$\ln X_{Mg_2Si_2O_6}^{cpX}/X_{Mg_2Si_2O_6}^{opX} = -\Delta H/RT + \Delta S/R = (-10202/T) + 5.35.$$

In light of new data discussed below, the Davis and Boyd diagram is now known to be erroneous and the Wood and Banno equation cannot be used in geothermometry. If the ΔG^{xs} versus T plot is done for the same solvus data (Fig. 1), it is evident that the inflection in this plot indicates that the solvus determination is erroneous. The inflection must represent either an undetected reaction or transformation, or simple inaccuracy in the data.

Since ΔH^{xs} and ΔS^{xs} are variable and the data plot is necessarily a curve, whether it is $\ln (X_1^A/X_1^B)$ versus $1/T$ or ΔG^{xs} versus T , a linear regression cannot represent the data with accuracy. A much more accurate equation would be afforded by a polynomial regression on ΔG^{xs} versus T . As an example the new data on the diopside-enstatite solvus at 30 kbar (Nehru and Wyllie, 1974; Mori and Green, 1975, 1976; Lindsley and Dixon, 1976) are plotted as points

in Figure 1. The data are excellently represented over the entire temperature range by a simple quadratic equation in T :

$$-RT \ln (X_{\text{Mg}_2\text{Si}_2\text{O}_6}^{\text{opx}} / X_{\text{Mg}_2\text{Si}_2\text{O}_6}^{\text{cpx}}) = \Delta G^{\text{xs}} = -4800 + 18.9T - 0.00829T^2.$$

An equation to be used in geothermometry should represent the system as accurately as possible. This is of more interest than approximate values of ΔH^{xs} and ΔS^{xs} . An equation obtained by polynomial regression should then be preferred to one obtained by linear regression for this purpose. The difficulty in using such an equation is that T appears on both sides. It can be overcome by using an equation derived by linear regression on $\ln (X_{\text{Mg}_2\text{Si}_2\text{O}_6}^{\text{cpx}} / X_{\text{Mg}_2\text{Si}_2\text{O}_6}^{\text{opx}})$ versus $1/T$ to obtain a rough temperature. This can then be refined in the quadratic equation by an iterative technique to obtain a more accurate solution. In either case, however, Lindsley and Dixon (1976) have indicated that the solvus data in this system are not of sufficient refinement for accurate geothermometry.

It should also be noted that these new data plotted in Figure 1 much more closely approximate a smooth curve than do the data of Davis and Boyd: they follow more closely the trend that solvus data must follow if there are no phase transformations or reactions. There is variance in the points from a smooth curve, but this is to be expected when one considers the remarks by all the aforementioned authors concerning the difficulties in obtaining equilibrium and accurate analysis by microprobe in this system. There are also limitations on the accuracy of pressure and temperature determinations with the high-pressure piston-cylinder apparatus which will contribute to this variance.

This type of plot has other useful aspects. If one extrapolates the curve to $\Delta G^{\text{xs}} = 0$,

$$-RT \ln X_1^{\text{A}} / X_1^{\text{B}} = (\mu_1^{\text{Axs}} - \mu_1^{\text{Bxs}}) = \Delta G^{\text{xs}} = 0; \quad (6)$$

$$\ln X_1^{\text{A}} / X_1^{\text{B}} = 0;$$

$$X_1^{\text{A}} = X_1^{\text{B}}.$$

In the case of trace-component distribution between two immiscible phases, one would expect equipartitioning of the component at the temperature obtained by extrapolation. In the case of binary solvus data, since there are only two components, complete solid solution should result:

$$X_2^{\text{A}} = 1 - X_1^{\text{A}} \quad \text{and} \quad X_2^{\text{B}} = 1 - X_1^{\text{B}};$$

$$X_1^{\text{A}} = X_1^{\text{B}};$$

$$X_2^{\text{A}} = 1 - X_1^{\text{A}} = X_2^{\text{B}}.$$

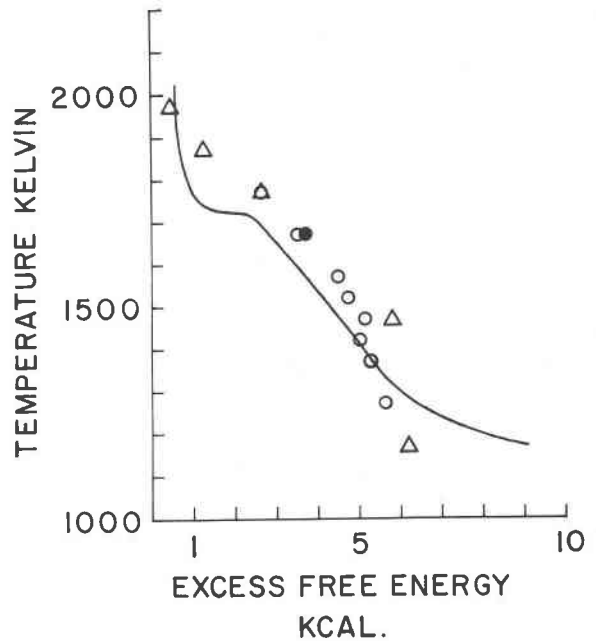


Fig. 1. The molar change in excess free energy of transferring $\text{Mg}_2\text{Si}_2\text{O}_6$ from the orthopyroxene to the clinopyroxene phase plotted against temperature. The solid line is calculated from the solvus of Davis and Boyd (1966). Open circles are from Nehru and Wyllie (1974); triangles from Mori and Green (1975 and 1976); and the closed circle from Lindsley and Dixon (1976). There are double datum points at 1673° and 1773°K .

These are of course subject to the condition that ΔG^{xs} is not affected appreciably by any increase in pressure which may be necessary to raise the solidus to the indicated temperature. The data may also be used to calculate activities. To illustrate this we may use the Davis and Boyd solvus at a temperature (1100°C), where it closely agrees with the later solvus determined by Nehru and Wyllie (1974). Since the enstatite phase contains very little diopside at all temperatures, we make the approximation that the chemical potential of $\text{Mg}_2\text{Si}_2\text{O}_6$ in it follows Raoult's law. As a result of this:

$$RT \ln a_{\text{Mg}_2\text{Si}_2\text{O}_6}^{\text{cpx}} = \Delta G^{\text{xs}} + RT \ln X_{\text{Mg}_2\text{Si}_2\text{O}_6}^{\text{opx}},$$

The ΔG^{xs} is about 5275 cal; the activity is 6.63, and the activity coefficient is 47.4.

The enstatite–diopside solvus may be further complicated in that the high-temperature $\text{Mg}_2\text{Si}_2\text{O}_6$ -rich diopside phase on the Davis and Boyd diagram is of the same composition as an "iron-free pigeonite" found by Kushiro (1969) at 20 kbar on the same join but at somewhat lower temperatures. Kushiro's identification was on the basis of X-ray diffraction. Davis and Boyd determined their solvus optically, and it

is not unreasonable to suspect that they may have mistaken one clinopyroxene for another. Warner and Luth (1974) also report a $P_{21/c}$ clinopyroxene at 1350°C and 1 kbar, and Eggler (1974) found pigeonite on the liquidus at 17 kbar in the system $\text{CaMgSi}_2\text{O}_6\text{-Mg}_2\text{SiO}_4\text{-SiO}_2$ under CO_2 -saturated conditions. However, Nehru and Wyllie (1974) investigated the enstatite–diopside solvus at 30 kbar and found no evidence of a “pigeonite” phase to 1500°C. Their solvus determination is supported by the subsequent work of Mori and Green (1975) and Lindsley and Dixon (1976). Mori and Green (1975) also investigated the solvus at 20 kbar and 1600°, and 30 kbar (1976) at 1600° and 1700°C. In each case they found no “pigeonite.” This greatly reduces the possible field of “pigeonite” to between 1500° and 1600°C at both 20 and 30 kbar. The diopside limb of the solvus as drawn by Mori and Green (1976) still retains a slight inflection in this temperature range at both pressures. The inflection in the solvus exhibits itself as a slight displacement of the highest temperature point toward a higher ΔG^{xs} than would be expected from the general trend in Figure 1. The point is calculated from the data of Mori and Green (1976), run Y2. I believe this point to be of questionable accuracy, because the diopside in that run had clearly not come to equilibrium as indicated by its broad range of composition. Mori and Green (1976) paired their enstatite with a diopside composition obtained by Howells and O'Hara (1975) for the same conditions.

It is concluded that excess functions are a more efficient convention than are activities for dealing with non-ideal solutions using the Nernst distribution equation. Plots of ΔG^{xs} versus T are shown to be a useful adjunct to the plots of $\ln(X_1^{\text{A}}/X_1^{\text{B}})$ versus T used by many authors dealing with trace-component distribution and geothermometry. They indicate more clearly discontinuities in the thermodynamic functions, which must be accompanied by phase transformations or reactions, and they are more adaptable to polynomial regressions which yield a more accurate representation of the system. Consideration of such a plot of data on the diopside–enstatite solvus at 30 kbar substantiates the conclusions that the original Davis and Boyd (1966) phase diagram is erroneous, and that the solvus is uninterrupted by phase transformations or reactions up to at least 1500°C. Above

1500°C a small “pigeonite” stability field may exist and further work is necessary to settle this.

Acknowledgments

I would like to express my appreciation to A. F. Koster van Groos and W. Visser for their invaluable discussion of the points presented in this paper and their guidance on proper exposition.

References

- Broecker, W. S. and V. M. Oversby (1971) *Chemical Equilibria in the Earth*. McGraw-Hill Book Co., New York.
- Carmichael, I. S., J. F. Turner and J. Verhoogen (1974) *Igneous Petrology*. McGraw-Hill Book Co., New York.
- Castellan, G. W. (1971) *Physical Chemistry*. Addison-Wesley Publishing Co., Reading, Mass.
- Davis, B. T. C. and F. R. Boyd (1966) The join $\text{Mg}_2\text{Si}_2\text{O}_6\text{-CaMgSi}_2\text{O}_6$ at 30 kilobars pressure and its application to pyroxenes from kimberlites. *J. Geophys. Res.*, 71, 3567–3576.
- Eggler, D. H. (1974) Effect of CO_2 on the melting of peridotite. *Carnegie Inst. Wash. Year Book*, 73, 215–224.
- Howells, S. and M. J. O'Hara (1975) Palaeogeotherms and the diopside–enstatite solvus. *Nature*, 254, 406–408.
- Kern, R. and A. Weisbrod (1967) *Thermodynamics for Geologists*. Freeman, Cooper and Co., San Francisco.
- Kushiro, I. (1969) The system forsterite–diopside–silica with and without water at high pressures. *Am. J. Sci.*, 267-A, 269–294.
- Lindsley, D. H. and S. A. Dixon (1976) Diopside–enstatite equilibria at 850°C to 1400°C, 5 to 35 kbar. *Am. J. Sci.*, 276, 1285–1301.
- Mori, T. and D. H. Green (1975) Pyroxenes in the system $\text{Mg}_2\text{Si}_2\text{O}_6\text{-CaMgSi}_2\text{O}_6$ at high pressure. *Earth Planet. Sci. Lett.*, 26, 277–286.
- and — (1976) Subsolidus equilibria between pyroxenes in the CaO-MgO-SiO_2 system at high pressures and temperatures. *Am. Mineral.*, 61, 616–625.
- Nehru, C. E. and P. J. Wyllie (1974) Electron microprobe measurement of pyroxenes coexisting with H_2O -undersaturated liquid in the join $\text{CaMgSi}_2\text{O}_6\text{-Mg}_2\text{Si}_2\text{O}_6\text{-H}_2\text{O}$ at 30 kilobars with applications to geothermometry. *Contrib. Mineral. Petrol.*, 48, 221–228.
- Swalin, R. A. (1972) *Thermodynamics of Solids*. John Wiley and Sons, New York.
- Thompson, J. B. (1967) Thermodynamic properties of simple solutions. In P. H. Abelson Ed., *Researches in Geochemistry II*, p. 340–361. John Wiley and Sons, New York.
- Warner, R. D. and W. C. Luth (1974) The diopside–orthoenstatite two-phase region in the system $\text{CaMgSi}_2\text{O}_6\text{-Mg}_2\text{Si}_2\text{O}_6$. *Am. Mineral.*, 59, 98–109.
- Wood, B. J. and S. Banno (1973) Garnet–orthopyroxene and orthopyroxene–clinopyroxene relationships in simple and complex systems. *Contrib. Mineral. Petrol.*, 42, 109–124.

Manuscript received, April 20, 1977; accepted for publication, August 24, 1977.